Fractal Electronics as a Generic Interface to Neurons

W.J. Watterson, S.M. Moslehi, J.H. Smith, R.D. Montgomery and R.P. Taylor
Physics Department, University of Oregon, Eugene, OR 97405, USA

Chapter in *The Fractal Geometry of the Brain* (Springer, 2016)

Imagine a world in which damaged parts of the body – an arm, or an eye, and ultimately a region of the brain – can be replaced by artificial implants capable of restoring or even enhancing human performance. The associated improvements in the quality of human life would revolutionize the medical world and produce sweeping changes across society. Biotechnology has the potential to transform this imagined world from science fiction into science fact. The use of implants to interface with the body is growing rapidly and represents the brave new world of electronics. However, today's electronic implants are based on the commercial electronics employed in computers and communications technology. Consequently, their performance is limited severely by the interface between the artificial and biological systems. In this chapter, we will discuss the optimal solution of establishing a bio-inspired interface using 'interconnects' that mimic the biological circuitry employed by the body – neurons. Neurons are fractal, featuring dendritic branches that repeat at increasingly fine sizes. We will discuss the construction of fractal interconnects and their fundamental functions – inducing and detecting electrical signals in the neurons. We will outline their enhanced performance, which includes their electrical, optical and physical properties.

Keywords: Fractals, bio-inspiration, human implants, electronics, neurons

Introduction

In 1752, Benjamin Franklin attached a metal key to the bottom of a dampened kite string and then flew the kite in a storm. It didn't take long to go from his simple demonstration of harnessing electricity to applying it to living bodies. In 1764, physician Charles Le Roy applied electricity to patients' eyes, causing them to see flashes of light. In 1791, Luigi Galvani did the same to the muscles of frog legs, causing them to twitch. Since then, two centuries of rapid development have led to today's commercial electronics industry. Miniaturization has been the main driver of improvements. In addition to faster operation, the evolution from micro-electronics to nano-electronics facilitates novel methods for manipulating the flow of electricity. For example, our research group has investigated ballistic electronics [1], quantum electronics [2], spin electronics [3] and coulomb blockade [4]. However, developments such as these target the computing and communications industry rather than electronic interfaces with biological systems.

Miniaturization offers surgeons the opportunity to implant devices in humans rather than relying on the crude external wires used by Le Roy and Galvini. For example, electronic devices have been implanted into human retinas in the hope of restoring vision to victims of retinitis pigmentosa and macular degeneration [5]. More than 80,000 Americans have brain implants designed to combat neurological disorders such as Parkinson's disease [6]. However, in each case the implant's functionality is limited by conventional designs inherited from the commercial electronics industry. For example, today's retinal implants could in principle deliver 20/80 vision and yet they only achieve 20/1260 vision, suggesting that they communicate with less than 10% of the targeted neurons [7]. Similarly, although research programs such as the White House BRAIN Initiative call for future electronics that simultaneously measure at least 10,000 neuronal signals, today's implants typically track less than 100 at a time [8].

Figure 1 highlights the fundamental mismatch between today's implants and the neurons that they interact with. Neurons are described by fractal geometry, featuring dendritic branches that repeat at increasingly fine size scales (Fig. 1a, b). In contrast, the active area of the implant is based on the smooth lines inherent in Euclidean geometry (for example, the grey square shape shown in Fig. 1c). Adopting the principle of bio-inspiration, we will describe the use of fractal interconnects to establish a 'biophilic' interface for the implants (Fig. 1d). In effect, the biophilic interface convinces nearby neurons that they are interacting with other neurons rather than an artificial device. We will consider implants with two distinct functions – stimulators (which induce electrical signals in the neurons) and sensors (which then detect and track these signals as they pass through the body's neural network). The superior electrical, optical and physical properties of the fractal interconnects are expected to be generic. Future applications could therefore include interaction with neurons in the brain, retina and limbs.

Fabrication of the Fractal Interconnects

When neurons interact with each other, they do so by exploiting both their physical and chemical environments. Our interconnects will do the same. In addition to adopting the physical geometry of the neurons, our project builds on previous

investigations of materials known to establish favourable chemical environments for the neurons. Accordingly, our fabrication methods exploit two established materials – TiN and carbon nanotubes (CNTs). TiN research demonstrates its stability over long periods of electronic operation both *in vitro* and *in vivo* [9]. *In vitro* neuron cultures on TiN reveal that it is also non-cytotoxic [10]. Furthermore, TiN retinal implants have been implanted in human patients for more than a year without negative reaction [11]. Similarly, the unique properties of CNTs make them ideal for bioelectronics. They have excellent electrical current capacity (1000 times greater than copper) and superior electron mobilities to silicon. They are also incredibly strong (100 times stronger than steel) yet mechanically flexible [12]. Furthermore, CNTs adhere well to substrates (with binding energies of a few eV/Å) [13] and living cells [14], and can be synthesized to be nontoxic [15]. For both material systems, we will adapt their surfaces to improve adhesion and the survival rate of the neurons. These procedures include using nanowire textures [16], homopolymer poly-L-lysine for TiN [9] and pyrene for the nanotubes [17].

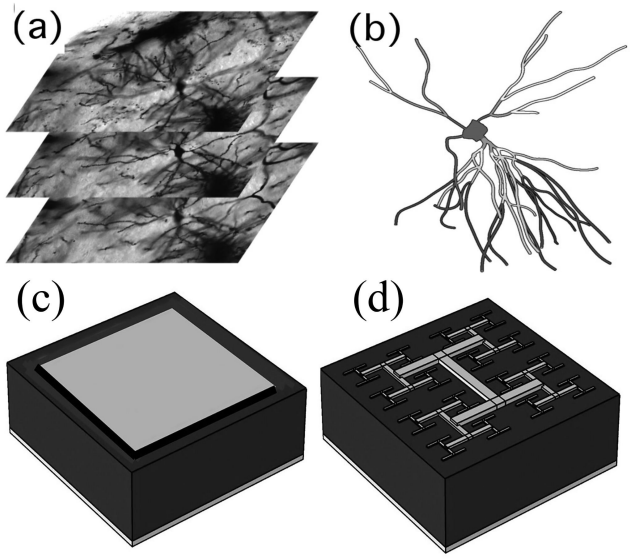

Figure 1. (a) In collaboration with B. Harland and J. Dalrymple-Alford (University of Canterbury, New Zealand), we use scanning confocal microscopy to image a stack of 200μm by 200μm horizontal sections (with vertical separations of 2μm) of Golgi-Cox stained neurons. (b) These sections are then computer-assembled into 3-dimensional images for pattern analysis. A neuron's basal dendrites from a rat's hippocampus are shown for demonstration. (c) A schematic showing the square-shaped active area (grey) of a conventional implant. (d) For our bio-inspired implants, the active area features branched patterns that repeat at different size scales.

Two novel fabrication techniques are being developed, each designed to match the fractal characteristics of the interconnects to those of the neurons. For each technique, the interconnects' smallest branches measure down to 50nm and the largest branches are designed to match the spread of the neuron branches – approximately 500μm for the brain and 20μm for the retina. Whereas all fractals exhibit repetition of patterns at multiple size scales, fractals can be grouped into two categories based on how the patterns repeat. For fractals prevalent in the body (e.g. neurons, veins and bronchial trees), the statistical qualities of the patterns repeat at different scales. In

contrast, the patterns of mathematically-generated 'exact' fractals repeat exactly at different scales. Consequently, whereas exact fractals look precisely the same at increasingly fine scales, 'statistical' fractals simply look similar at different scales [18]. One of our fabrication techniques exploits the precision and control associated with the clean geometry of exact fractals. The other harnesses natural growth processes to generate statistical fractals similar to neurons. Fractal dimension D is a central parameter for quantifying both types of fractal. This describes how the patterns occurring at different scales combine to build the resulting fractal shape [18]. For Euclidean shapes, dimension is described by familiar integer values – for a smooth line $D = 1$, while for a completely filled area $D = 2$. However, the repeating patterns of a fractal line cause the line to begin to occupy more space. Consequently, its D value lies between 1 and 2. Figure 2a,b shows the result of adjusting D for the branches of our fractal interconnects. For each fabrication method, D can be adjusted along with the number of repeating iterations I to investigate the impact of these fractal parameters on the interconnects' properties.

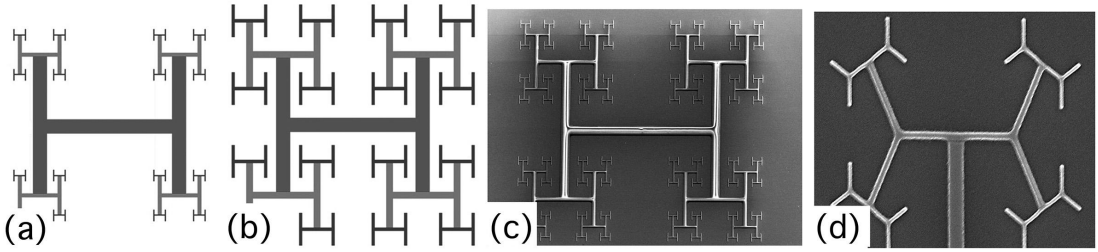

Figure 2. (a, b) Schematic demonstrations of D's impact on the scaling properties of an exact interconnect in which an 'H' pattern repeats. Three iterations of repetition are shown. Note how the H's size decreases at a higher rate between iterations for $D = 1.1$ (shown in (a)) than for $D = 1.9$ (shown in (b)). (c, d) Scanning electron micrographs (SEMs) of interconnects featuring $D = 1.5$ branches made in collaboration with K. Fairley and D. Johnson (University of Oregon, USA). The branches span from 500μm down to 2μm in (c). In (d), the widths of the smallest branches are ~10 nm.

The exact fractal interconnects (Fig. 2) are fabricated using electron-beam lithography [19] to generate patterns in two bio-compatible resists (SU-8 and HafSOx). For the SU-8 method, this pattern can then be transferred to a TiN pattern using electron-beam evaporation and a 'lift-off' technique. For the HafSOx method, the exposed HafSOx acts as a mask for an electron milling process that defines the pattern in an underlying TiN layer.

Fabricated using novel self-assembly growth processes, the statistical fractal interconnects look strikingly similar to neurons (Fig. 3). Using this technique, a beam of metallic clusters (each with a diameter of ~50nm) is deposited on a substrate in an ultra high vacuum chamber. These clusters then grow into fractal islands called nanoflowers by diffusion-limited aggregation [20]. Figure 3a charts this growth process, showing the small ellipsoidal islands that initially form (plotted on the graph's left side) and the islands with fractal branches that they grow into (right side). The islands' fractal morphology can be adjusted by varying deposition conditions such as temperature, deposition rate and flux (Figs. 5b – d). Fortuitously, neighbouring islands naturally self-avoid rather than merge (Fig. 5c), allowing arrays of fractal interconnects to be grown efficiently.

Figure 3e shows statistical fractals formed from CNTs that spread both parallel and perpendicular to the implant's surface with thicknesses of ~1μm. Both single and multi-walled varieties of the nanotubes are synthesized using chemical vapour deposition. In this process, substrates are metallized with thin (a few Å) layers of a catalyst (e.g. Fe, Co) that form a network of metallic islands. These islands then serve as seeds for nanotube growth, allowing them to connect to multiple catalyst islands and form a large network called a CNT 'mat'. These growth conditions are being manipulated to generate statistical fractal interconnects. To achieve higher degrees of fractal quality of the CNT networks, the catalyst islands can be patterned using optical or electron-beam lithography, or the mat can be patterned post-synthesis by etching away selected regions. An alternative approach for etching will be pursued using atomic force microscopy (AFM). The sharp tip of the AFM will be scanned across the nanotube network while applying an electrical bias to the probe tip, which will cut the network into the desired fractal pattern. Both approaches can achieve features with 10nm resolution.

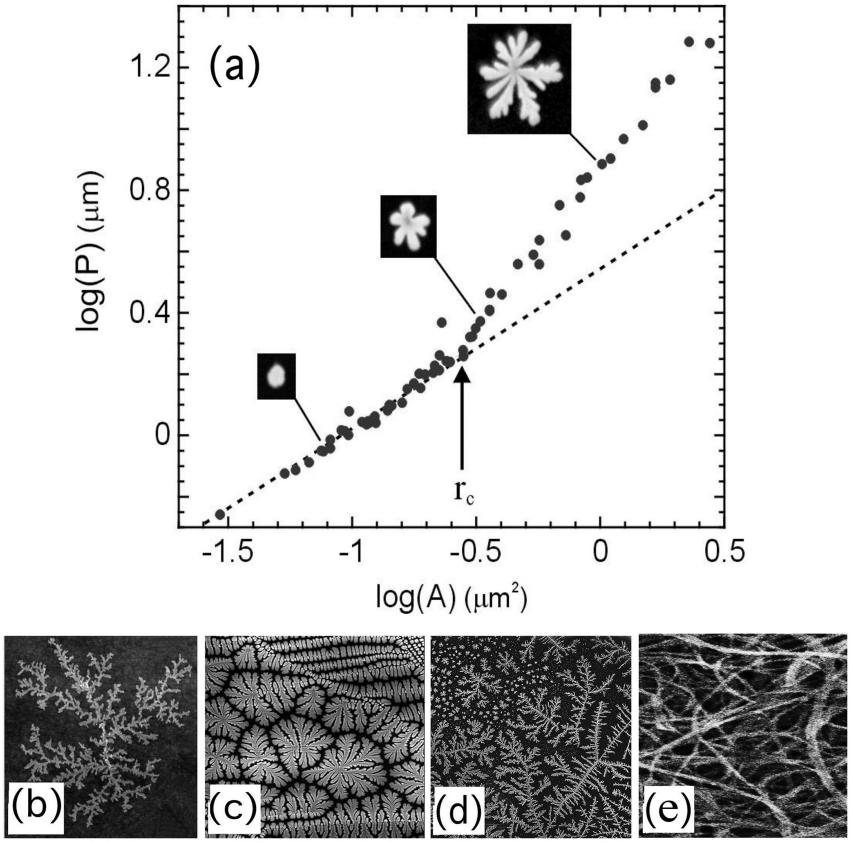

Figure 3 (a) A plot of log (island perimeter *P*) versus log (island area *A*), as measured from a digital SEM image. Each data point represents an individual island. The dotted line is a guide to the eye, showing the behaviour expected for purely ellipsoidal (i.e. non-fractal) islands. The critical radius (r_c) represents the point at which the data deviates from this behaviour, indicating the formation of fractal branches. (b-c) Images of fractal interconnects demonstrating that their fractal morphology can be controlled by the growth conditions. The interconnects in (b, c) are 10μm wide. In (d), fractal features span a remarkable 2.5 orders of magnitude down to 90nm. The interconnects shown in (a-d) are fabricated in collaboration with S. Brown (University of Canterbury, New Zealand). (e) A SEM showing a 5μm section of a network of CNT branches fabricated in collaboration with B. Alemán (University of Oregon, USA).

Functionality of the Fractal Interconnects

Our implants are designed to serve two distinct electronics functions – inducing and detecting electrical signals in the neurons. For both functionalities, it is crucial to consider the impact of the fractal design on the mechanical, optical, electrical and physical (adhesive) properties of the neuron-implant interface. Adopting the philosophy that the implant is only as strong as its weakest link, we are targeting the fundamental science that emerges when all of these properties are considered in unison. In terms of their mechanical properties, fractal circuits were recently proposed for stretchable electronics [21] – the associated flexibility will therefore allow our interconnects to be conformal to the regions in which they are implanted. In terms of optics, the surface coverage of the fractal interconnects is considerably less than the equivalent squares due to the multitude of gaps between the branches (Fig.1c, d). This suggests that light can be easily transmitted through the fractal interconnect. This will be advantageous for future brain implants that ultilize both optical and electrical stimulation [22]. Furthermore, the ability to shine light through the interconnects is crucial for the operation of retinal implants [5]. In addition to minimizing coverage, some of the fractal branches are comparable to, or smaller than, the light's wavelength. This raises the possibility of manipulating feature sizes to tune the light transmission using diffractive and plasmonic effects. This idea is inspired by recent experiments (unrelated to implants) demonstrating that fractal branches efficiently filter light based on its wavelength [23]. The fractal interconnects could therefore potentially serve as colour filters, allowing them to receive white light and then selectively transmit red, green and blue light. As an example of applications, this 'RGB' sensitivity could be used to build the first colour vision implants (today's retinal implants generate monochromatic vision).

The interconnects' electrical properties are crucial to the operation of both stimulators and sensors. Electronic stimulation dates back to the pioneering *in vivo* studies of Le Roy and Galvini. The electrical fields from their electrodes set up potential differences across the neuron membrane, inducing ion flows that triggered a signal along the axon [24]. In Le Roy's experiment for example, this process induced signals in the retinal neurons that the brain interpreted as originating from the retina's photoreceptors. The positive impact of adopting the fractal geometry becomes clear by returning to the schematic of Fig. 1c,d in which the grey interconnect serves as the stimulating electrode. For the same surface coverage, the fractal geometry spreads out further across the implant's surface than for the conventional square design (i.e. its bounding perimeter is larger). Consequently, the voltages induced by the interconnect extend further from the implant surface into the neural layer and these larger distances rapidly increase the likelihood of stimulation. The precise extent to which the fractal interconnect out-performs the square will depend on its *D* value (Fig. 2a, b).

In terms of electronic sensors, today's conventional implants employ either multiple electrode arrays (MEAs) or multiple transistor arrays (MTAs) to measure the electrical potentials generated by neuron signals. However, the simultaneous occurrence of many neuronal signals makes tracking individual signals extremely difficult. This problem is analogous to the 'cocktail party problem' when the listener tries to focus on a specific conversation among the background 'chatter' from many guests. To accomplish this task, recordings from the conventional sensors are

analyzed using waveform analysis or triangulation to determine signal location. Waveform analysis relies on *a priori* information about signals' temporal characteristics (their waveforms) to identify unique signatures of individual neurons. *In vivo*, this is limited by: 1) isolating thousands of signals, 2) waveform variability within each neuron, and 3) electrode drift with time [25]. Triangulation works by measuring the waveform variation between different sensors in the array. However, errors in uniquely identifying thousands of signals present critical problems for triangulation algorithms [26]. Despite the clear need to develop non-subjective measures of signals with quantified errors, different laboratories still can't objectively compare data. Our fractal sensor avoids all of the above limitations by uniquely identifying neuronal signals without post-measurement analysis and its reliance on *a priori* information about waveforms. Our probe achieves this by adopting the MTA approach but taking the vital step of incorporating a fractal conduction network.

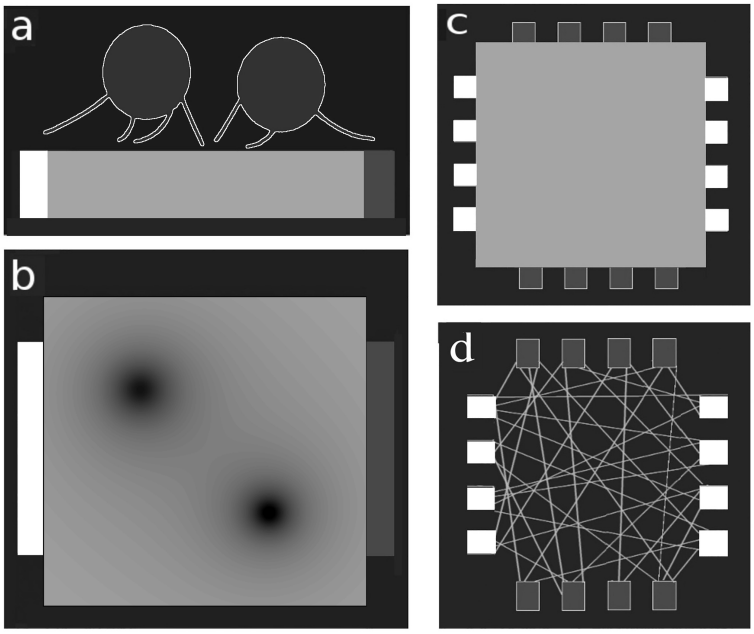

Figure 4. (a) A side-view of a FET sensor. The neurons (outlined in white) generate signals that are detected by measuring the electricity flowing through the channel (light grey) between the source (white) and drain (dark grey) terminals. (b) A top view of the FET. The neuron signal depletes electrons in the channel regions (dark) directly below the neurons, thus reducing the measured current flow. (c) A modified FET using multiple (16) sources and drain terminals. (d) A FET based on a statistical fractal network of CNTs (light grey lines).

For the conventional MTA, each field effect transistor (FET) in the array features a silicon channel (light grey) which conducts electricity between source (white) and drain (dark grey) terminals (Fig. 4a, b). The electric potential generated by neuron signals depletes electrons in the channel, leading to a measurable resistance change. Unfortunately, this traditional design offers little flexibility for improvement. For example, gains in measurement resolution by reducing device size are inevitably coupled with larger measurement noise due to increased resistance. Our bio-inspired design is shown in Fig. 4d. Current is passed from each of the source terminals (white) to each of the drains (dark grey) through a fractal distribution of conducting channels (light grey lines). Depletion of a local region of this network will induce a

re-arrangement of current through the network. The non-linear signature of this re-arrangement produces an exponential sensitivity of the measured resistance to the location of the depletion region [20] and hence to the neuronal signal. To detect the non-linear signature, the number of measurement terminals per transistor is increased from two for the conventional FET (Fig. 4a, b) to 16 (Fig. 4d). These combine to create an emergent knowledge greater than the sum of the individual measurements. This is achieved through a calibration library that, in real time, converts the multiple resistance values into unique values for position and size of each signal's depletion pattern. The library is generated by a systematic series of tests which establish the unique multi-resistance signatures of different neuron signal positions. Returning to the cocktail party analogy, the resulting enhanced sensitivity is equivalent to giving the party guests hearing aids. The calibration library is equivalent to the guests working as a team, comparing notes about previous parties.

The Biophilic Interface

Building on the advantageous mechanical, optical and electrical properties outlined so far, the fractal network also provides a crucial bio-inspired function by establishing a physical fractal pattern in the implant surface. This encourages neurons to stay close to the surface, enhancing stimulation and detection of their signals. This is analogous to attracting the party guests that you want to listen and talk to. Previous experiments have shown that surface topologies that are not smooth encourage neuron adhesion e.g. [16, 27-30] and that topological factors are more important than the chemical environment established by the materials used [31]. Only 10% of neurons adhere to smooth metallic interconnects [11] while experiments on textured metallic interconnects indicate 50% [32]. None of the previous studies took the vital step of introducing surface patterns that match the neurons' fractal branches to improve adhesion.

In addition, smooth surfaces are known to trigger an accumulation of glial cells into a protective layer called a glial scar [33]. Whereas the presence of individual glial cells is a signature of health (because they serve as the neuron's life-support system), the scar pushes the neurons away from the smooth surface of conventional implants reducing their ability to stimulate or sense the neurons. Based on these findings, our *in vitro* experiments (Fig. 5) are designed to test our hypothesis that: 1) neurons will adhere to the physical patterns established by the fractal distribution of channels (i.e. the pattern of lines in Fig. 4d), 2) to maintain health, these neurons might be accompanied by individual glial cells, 3) glial cells will accumulate in the smooth regions established by the larger gaps (i.e. black regions) in Fig. 4d. Thus, even if this accumulation eventually forms a scar, it will not form on the lines (conducting channels).

In the *in vitro* experiments, implants are lowered into a retinal culture and fluorescence microscopy is used to image cells as they interact with the interconnects [34]. To prepare the culture, the retina is first removed from the outer epithelium of neonatal mice and placed in a culture medium, which is then mechanically agitated to separate the retinal cells. Staining allows the various retinal cells to be analysed separately. DAPI (blue) fixes to both glia and neuron cell nuclei (allowing a total cell count), GFAP (green) attaches to glia cells, and β-tubulin III (red) binds to neuron microtubules. A simple test geometry, consisting of rows of 100μm-wide textured regions separated by rows of smooth surface, confirmed expectations that neurons

predominantly adhere to the textured regions and glial cells accumulate in the smooth gaps [35]. Furthermore, immunohistochemistry confirmed that markers expressed by healthy neurons were present. The microscopy was performed after 18 days (this is close to the maximum period for *in vitro* studies). This time frame is significantly longer than on-sets of scar formation in previous *in vitro* experiments (2 days) [36] and is of the order of scar formation in *in vivo* experiments (2-3 weeks) [37]. Thus, any detrimental developments would have emerged by day 18. Furthermore, there were no significant changes between days 8 and 18, suggesting the experiment captured long-term behaviour and that the observed positive effects will persist indefinitely.

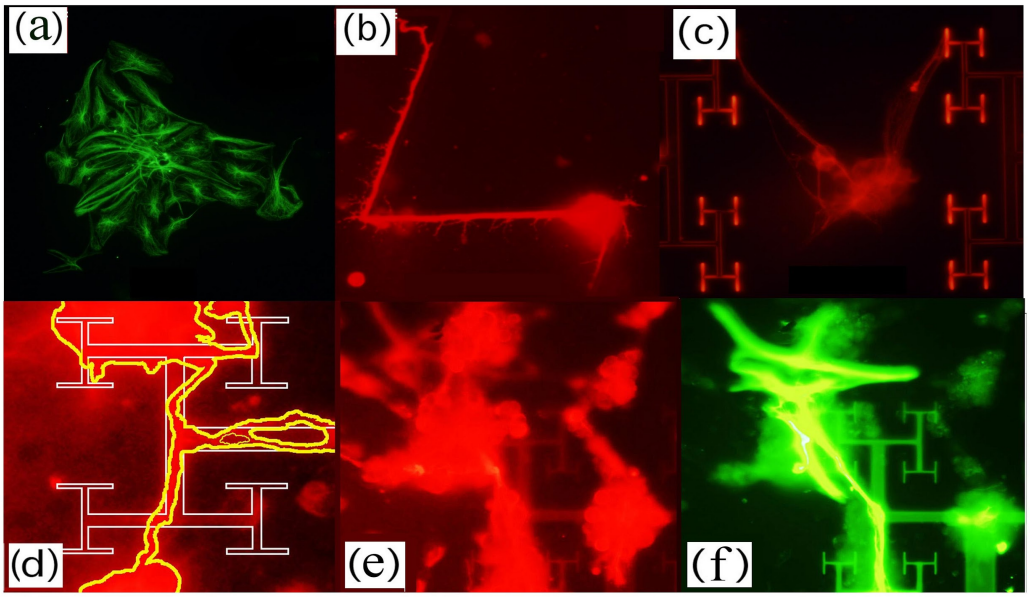

Figure 5. Images from the *in-vitro* fluorescence microscopy experiments. (a) A 300µm-wide glial scar (green) forming on a smooth surface. (b) A neuron (red) extending along a test interconnect with a 200µm long 'zig-zag' shape. (c) A neuron (red) located in a 100µm gap within one of our fractal 'H-tree' designs. (d) Individual neuron dendrites (highlighted with yellow edges) attach to fractal interconnect branches (white edges) (image width = 60µm). The images in (e) and (f) demonstrate how individual neurons (red) and glial cells (green) adhere to the same interconnect region (image widths = 150µm). All images are taken in collaboration with M.T. Perez (Lund University, Sweden).

Figure 5a shows an image of glial cells (green) accumulating on a smooth surface and forming a scar. We are developing novel pattern analysis techniques to characterize this process and to quantify the scar's growth rate and size. The image in Fig. 5b shows a neuron (red) extending along a test interconnect with a zig-zag shape. These test patterns show that neurons can follow interconnect branches for more than 200µm and can turn through angles sharper than 90 degrees. The image in Fig. 5c shows a neuron located in a gap within one of our fractal 'H-tree' designs. Images such as this are being used to quantify how far neuron dendrites can extend in order to adhere to the interconnect branches. The interconnect's fractal geometry amplifies the effects revealed in Figs. 5a-c because it maximizes the combination of patterned lines and smooth gaps within a given region. Indeed, positive effects are already evident after 3 days in culture: the zoom-in of Fig. 5d shows adhesion of neural dendrites to

the fractal lines of the interconnect. This picture is further supported by Fig. 5e,f which show that an attached neuron is accompanied by an individual glial cell.

Based on the above preliminary research, our long-term aim is for each neuron dendrite to automatically seek out and adhere to a fractal branch of the interconnect. Consequently, this 'one-to-one' adhesion could generate unprecedented stimulation and sensing. We also aim for 'selective' adhesion, whereby targeted types of neuron will adhere to specific interconnects. We hope to achieve selective adhesion (and consequently selective stimulation and sensing) by matching the specific fractal properties of the interconnects to those of the target neurons. Analysing the neuron shapes is vital for understanding the neuron-interconnect interface. Previous research of neuron geometry used fractal analysis simply as a tool for quantifying their structural complexity. In contrast, we are using confocal microscopy to construct 3-dimensional images of neurons, allowing the first investigation of the origin of neurons' fractal character (Fig. 1a, b). Strikingly, this character originates from the way dendrites 'weave' though space. This has crucial consequences because adhesion experiments reveal that this weave is forced to change as neurons interact with surfaces. Our hypothesis predicts superior adhesion when the fractal characteristics (in particular D and branch orientation (Fig. 2)) of the interconnect and neuron are matched. This will occur because the dendrites can connect without having to adjust their fractal characteristics. This effect is an example of 'fractal geometric resonance' in which interface properties are enhanced by matching the geometric properties of two fractals. Because different neuron types are expected to have specific weaves [38], selective adhesion should be possible – whereby specific neurons adhere to targeted interconnects based on their precise fractal characteristics. This novel capability offers the possibility of revolutionizing applications of human implants. Considering the eye as an example, the retina features five types of neuron. Successful implants will need to select which neuron types to stimulate and sense. Similarly, brain implants will also be able to target selected neuron types.

Conclusions

Fractal implants that stimulate or sense neuronal signals in the brain could be used to address a number of pathological conditions including Parkinson's disease. In addition, they could also radically improve other stimulation techniques to improve learning and cognition, visual perception, working memory, and motor control [39]. The long-term potential impact of fractal interconnects stretches well beyond improving implants designed to interact with the human brain, retina and limbs. In addition to stimulating and sensing naturally occurring neurons, they could be applied to retinal STEM cells in *in vitro* and *in vivo* investigations.

Acknowledgments

We thank our collaborators S. Brown, J. Dalrymple-Alford and B. Harland (University of Canterbury, New Zealand), B. Alemán, K. Fairley and D. Johnson (University of Oregon, USA), and M. Perez (Lund University, Sweden). We also thank the Research Corporation for Science Advancement (RCSA), the ONR–ONAMI N3 program and the W.M. Keck Foundation for funding.

References

[1] See AM, Pilgrim I, Scannell BC, Montgomery R, Klochan O, Aagesen M, Lindelof P, Farrer I, Ritchie DA, Taylor RP, Hamilton AR and Micolich AP. Impact of small-angle scattering on ballistic transport in quantum dots. Physical Review Letters. 2012; 108: 196807 –10.

[2] Micolich AP, Taylor RP, Davies AG, Bird JP, Newbury R, Fromhold TM, Ehlert A, Linke H, Macks LD, Tribe WR, Linfield EH, Ritchie DA, Cooper J, Aoyagi Y and Wilkinson PB. The evolution of fractal patterns during a classical-quantum transition. Physical Review Letters. 2001; 87: 036802-5.

[3] Sachrajda AS, Taylor RP, Dharma-Wardana D, Zawadski P, Adams JA and Coleridge PT. Spin-controlled resonances in the magneto-transport in quantum dots. Physical Review B Rapid Communications. 1993; 47: 6811-4.

[4] Taylor RP, Sachrajda AS, Zawadzki P, Coleridge PT and Adams JA. Aharonov-Bohm oscillations in the coulomb blockade regime. Physical Review Letters. 1992; 69: 1989-92.

[5] Zrenner E. Will retinal implants restore vision?. Science. 2002; 295:1022-5.

[6] Lozano A. Tuning the brain. The Scientist. 2013; 27. Available from: http://www.the-scientist.com/?articles.view/articleNo/38047/title/Tuning-the-Brain/

[7] Taylor RP. Artificial vision: vision of beauty. Physics World. 2011; 24: 22-7.

[8] Abbot A. Neuroscience: Solving the brain. Nature. 2013; 499: 272-4.

[9] Hämmerle H, Kobuch K, Kohler K, Nisch W, Sachs H, Stelzle M. Biostability of micro-photodiode arrays for subretinal implantation. Biomaterials. 2002; 23:797-804

[10] Guenther E, Tröger B, Schlosshauer B, Zrenner E. Long-term survival of retinal cell cultures on retinal implant materials. Vision research. 1999; 39: 3988-94.

[11] Stingl K, Bartz-Schmidt KU, Besch D, Chee CK, Cottriall CL, Gekeler F, Groppe M, Jackson TL, MacLaren RE, Koitschev A, Kusnyerik A. Subretinal Visual Implant Alpha IMS–Clinical trial interim report. Vision research. 2015; 111: 149-60.

[12] Jensen K, Mickelson W, Kis A, Zettl A. Buckling and kinking force measurements on individual multiwalled carbon nanotubes. Physical Review B. 2007; 76: 195436.

[13] Hertel T, Walkup RE, Avouris P. Deformation of carbon nanotubes by surface van der Waals forces. Physical Review B. 1998; 58:13870.

[14] Fischer KE, Alemán BJ, Tao SL, Daniels RH, Li EM, Bünger MD, Nagaraj G, Singh P, Zettl A, Desai TA. Biomimetic nanowire coatings for next generation adhesive drug delivery systems. Nano letters. 2009; 9: 716-20.

[15] Liu Y, Zhao Y, Sun B, Chen C. Understanding the toxicity of carbon nanotubes. Accounts of Chemical Research. 2012; 46: 702-13.

[16] Hällström W, Mårtensson T, Prinz C, Gustavsson P, Montelius L, Samuelson L, Kanje M. Gallium phosphide nanowires as a substrate for cultured neurons. Nano letters. 2007; 7: 2960-5.

[17] Chen X, Kis A, Zettl A, Bertozzi CR. A cell nanoinjector based on carbon nanotubes. Proceedings of the National Academy of Sciences. 2007; 104: 8218-22.

[18] Fairbanks MS, Taylor RP. Measuring the scaling properties of temporal and spatial patterns: From the human eye to the foraging albatross. Nonlinear Dynamical Systems Analysis for the Behavioral Sciences Using Real Data. 2011: 341-66.

[19] Taylor RP. The role of surface-gate technology for AlGaAs/GaAs nanostructures. Nanotechnology. 1994; 5: 183.

[20] Fairbanks MS, McCarthy DN, Scott SA, Brown SA, Taylor RP. Fractal electronic devices: simulation and implementation. Nanotechnology. 2011; 22: 365304.

[21] Fan JA, Yeo WH, Su Y, Hattori Y, Lee W, Jung SY, Zhang Y, Liu Z, Cheng H, Falgout L, Bajema M. Fractal design concepts for stretchable electronics. Nature communications. 2014; 5.

[22] Zhang J, Laiwalla F, Kim JA, Urabe H, Van Wagenen R, Song YK, Connors BW, Zhang F, Deisseroth K, Nurmikko AV. Integrated device for optical stimulation and spatiotemporal electrical recording of neural activity in light-sensitized brain tissue. Journal of neural engineering. 2009; 6: 055007.

[23] Afshinmanesh F, Curto AG, Milaninia KM, van Hulst NF, Brongersma ML. Transparent metallic fractal electrodes for semiconductor devices. Nano letters. 2014; 14: 5068-74.

[24] Cogan SF. Neural stimulation and recording electrodes. Annual Review Biomedical Engineering. 2008; 10: 275-309.

[25] Einevoll GT, Franke F, Hagen E, Pouzat C, Harris KD. Towards reliable spike-train recordings from thousands of neurons with multielectrodes. Current opinion in neurobiology. 2012; 22: 11-7.

[26] Buzsáki G. Large-scale recording of neuronal ensembles. Nature neuroscience. 2004; 7: 446-51.

[27] Rajnicek A, Britland S, McCaig C. Contact guidance of CNS neurites on grooved quartz: influence of groove dimensions, neuronal age and cell type. Journal of cell science. 1997; 110: 2905-13.

[28] Fan YW, Cui FZ, Hou SP, Xu QY, Chen LN, Lee IS. Culture of neural cells on silicon wafers with nano-scale surface topograph. Journal of neuroscience methods. 2002; 120: 17-23.

[29] Gentile F, Medda R, Cheng L, Battista E, Scopelliti PE, Milani P, Cavalcanti-Adam EA, Decuzzi P. Selective modulation of cell response on engineered fractal silicon substrates. Scientific reports. 2013; 3.

[30] Mattson MP, Haddon RC, Rao AM. Molecular functionalization of carbon nanotubes and use as substrates for neuronal growth. Journal of Molecular Neuroscience. 2000; 14: 175-82.

[31] Gomez N, Chen S, Schmidt CE. Polarization of hippocampal neurons with competitive surface stimuli: contact guidance cues are preferred over chemical ligands. Journal of The Royal Society Interface. 2007; 4: 223-33.

[32] Schlie-Wolter S, Deiwick A, Fadeeva E, Paasche G, Lenarz T, Chichkov BN. Topography and coating of platinum improve the electrochemical properties and neuronal guidance. ACS applied materials & interfaces. 2013; 5: 1070-7.

[33] Butterwick A, Huie P, Jones BW, Marc RE, Marmor M, Palanker D. Effect of shape and coating of a subretinal prosthesis on its integration with the retina. Experimental Eye Research. 2009; 88: 22-9.

[34] Piret G, Perez MT, Prinz CN. Neurite outgrowth and synaptophysin expression of postnatal CNS neurons on GaP nanowire arrays in long-term retinal cell culture. Biomaterials. 2013; 34: 875-87.

[35] Piret G, Perez MT, Prinz CN. Support of Neuronal Growth Over Glial Growth and Guidance of Optic Nerve Axons by Vertical Nanowire Arrays. ACS applied materials & interfaces. 2015; 7: 18944-8.

[36] Lewis GP, Fisher SK. Muller cell outgrowth after retinal detachment: association with cone photoreceptors. Injury. 2000; 1542: 1545.

[37] Polikov VS, Tresco PA, Reichert WM. Response of brain tissue to chronically implanted neural electrodes. Journal of neuroscience methods. 2005; 148: 1-8.

[38] MacNeil MA, Heussy JK, Dacheux RF, Raviola E, Masland RH. The population of bipolar cells in the rabbit retina. Journal of Comparative Neurology. 2004; 472: 73-86.

[39] Fox D. Neuroscience: brain buzz. Nature News. 2011; 472: 156-9.